Orientation-Controlled Growth of Single-Crystal Silicon-Nanowire Arrays

ARTICLE *in* ADVANCED MATERIALS · JANUARY 2005

Impact Factor: 17.49 · DOI: 10.1002/adma.200400474

6 AUTHORS, INCLUDING:

Yanguo Chen
Texas A&M University
517 PUBLICATIONS **9,915** CITATIONS
SEE PROFILE

Rongming Wang
University of Science and Technology Beijing
169 PUBLICATIONS **4,436** CITATIONS
SEE PROFILE

ADVANCED MATERIALS

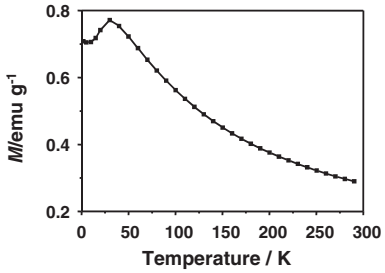

Figure 4. Magnetization (M) of the ZFC mesostructured Co_3O_4, in an applied field of 1.0 T, as a function of temperature.

is higher than that observed for Co_3O_4 with an average particle size of 20 nm (25 K).[11] This is in accordance with the smaller average particle size, which corresponds to a higher fraction of surface spins, and hence for which bulk behavior is expected to occur at higher temperatures. Relationships between block temperature and particle size have also been studied for Mn_3O_4 and γ-Fe_2O_3, and the peak temperature was also found to increase with decreasing particle size.[12]

In conclusion, mesostructured Co_3O_4 with *Ia3d* symmetry has been nanocast from cubic *Ia3d* mesoporous vinylsilica. The vinyl groups play an important role in entrapping $Co(NO_3)_2$ inside the pores. This process seems to be extendable to other metal oxides. The cobalt oxide synthesized has interesting magnetic properties, and may be the basis of magnetic nanocomposites, if the pore system can be filled with another ferromagnetic material. It will be very interesting to see what kind of magnetic properties result from the interaction of two different, ordered, ferromagnetic structures on a nanometer size scale.

Experimental

0.5 g of vinyl-functionalized silica (synthesized using 20 % vinyltriethoxysilane and aged at 100 °C [4], hereafter called vinylsilica) was soaked in 5 mL of 0.8 M $Co(NO_3)_2$ ethanolic solution, dried at 200 °C, re-impregnated, and then calcinated at 450 °C for 6 h. The amount of cobalt oxide in the composite was then typically 50–55 wt.-%. The silica was then dissolved in a 2 M NaOH aqueous solution, with the NaOH solution being replaced 3 times. The samples were characterized using standard techniques, such as XRD, N_2 sorption analysis, and TEM. The magnetic properties were measured using a superconducting quantum interference device (SQUID).

Received: May 17, 2004
Final version: September 2, 2004
Published online: November 22, 2004

[1] a) F. Schüth, *Chem. Mater.* **2001**, *13*, 3184. b) G. J. de A. A. Soler-Illia, C. Sanchez, B. Lebeau, J. Patarin, *Chem. Rev.* **2002**, *102*, 4093.
[2] See the following reviews: a) F. Schüth, *Angew. Chem. Int. Ed.* **2003**, *42*, 3604. b) C. Z. Yu, B. Z. Tian, D. Y. Zhao, *Curr. Opin. Solid State Mater. Sci.* **2003**, 7, 191. c) R. Ryoo, S. H. Joo, *Stud. Surf. Sci. Catal.* **2004**, *148*, 241.
[3] R. Ryoo, S. H. Joo, S. Jun, *J. Phys. Chem. B* **1999**, *103*, 7743.
[4] a) H. J. Shin, R. Ryoo, Z. Liu, O. Terasaki, *J. Am. Chem. Soc.* **2001**, *123*, 1246. b) F. Kleitz, S. H. Choi, R. Ryoo, *Chem. Commun.* **2003**, *17*, 2136.
[5] P. Poizot, S. Laruelle, S. Grugeon, L. Dupont, J. M. Tarascon, *Nature* **2000**, *407*, 496.
[6] a) B. Z. Tian, X. Y. Liu, H. F. Yang, S. H. Xie, C. Z. Yu, B. Tu, D. Y. Zhao, *Adv. Mater.* **2003**, *15*, 1370. b) B. Z. Tian, X. Y. Liu, L. A. Solovyov, Z. Liu, H. F. Yang, Z. Zhang, S. H. Xie, F. Q. Zhang, B. Tu, C. Z. Yu, O. Terasaki, D. Y. Zhao, *J. Am. Chem. Soc.* **2004**, *126*, 865.
[7] Y. Q. Wang, C. M. Yang, B. Zibrowius, B. Spliethoff, M. Lindén, F. Schüth, *Chem. Mater.* **2003**, *15*, 5029.
[8] M. Kaneda, T. Tsubakiyama, A. Carlsson, Y. Sakamoto, T. Ohsuna, O. Terasaki, S. H. Joo, R. Ryoo, *J. Phys. Chem. B* **2002**, *106*, 1256.
[9] S. Jun, S. H. Joo, R. Ryoo, M. Kruk, M. Jaroniec, Z. Liu, T. Ohsuna, O. Terasaki, *J. Am. Chem. Soc.* **2000**, *122*, 10 712.
[10] a) P. I. Ravikovitch, A. V. Neimark, *Langmuir* **2000**, *16*, 2419. b) K. Schumacher, P. I. Ravikovitch, A. D. Chesne, A. V. Neimark, K. K. Unger, *Langmuir* **2000**, *16*, 4648.
[11] S. I. Makhlouf, *J. Magn. Magn. Mater.* **2002**, *246*, 184.
[12] a) W. S. Seo, H. H. Jo, K. Lee, B. Kim, S. J. Oh, J. T. Park, *Angew. Chem. Int. Ed.* **2004**, *43*, 1115. b) T. Hyeon, S. S. Lee, J. Park, Y. Chung, H. B. Na, *J. Am. Chem. Soc.* **2001**, *123*, 12 798.

Orientation-Controlled Growth of Single-Crystal Silicon-Nanowire Arrays**

By *Shuaiping Ge*, *Kaili Jiang*,* *Xiaoxiang Lu*, *Yaofeng Chen*, *Rongming Wang*, and *Shoushan Fan**

Development in the integrated-circuit (IC) industry is directed towards creating smaller and faster components that consume less power.[1] Owing to their unique structures and properties, one-dimensional nanoscale objects have shown many promising potential applications in future nanoscale electronics[2–4] and photonics applications.[2,5,6] Since the IC industry is currently dominated by silicon-based devices, silicon nanowires (SiNWs) will have the advantage of technical compatibility, compared with other semiconducting nanowires. Recently, many efforts have been directed towards the growth of SiNWs.[7,8] However, most of these methods give

[*] Prof. K. Jiang, Prof. S. Fan, S. Ge, X. Lu
Department of Physics and
Tsinghua–Foxconn Nanotechnology Research Center
Tsinghua University
Beijing 100084 (P. R. China)
E-mail: jiangkl@tsinghua.edu.cn, fss-dmp@tsinghua.edu.cn
Y. Chen, Prof. R. Wang
Electron Microscopy Laboratory and
State Key Laboratory for Mesoscopic Physics
School of Physics
Peking University
Beijing 100087 (P. R. China)

[**] This work was supported by the National Natural Science Foundation of China, the State Key Project of Fundamental Research of China, and the Natural Science Foundation of Beijing (3012007). Supporting Information is available online from Wiley InterScience or from the author.

  DOI: 10.1002/adma.200400474

rise to randomly oriented SiNWs, which require further assembling procedures to make devices on substrates.[3,5] The control of the orientations of the SiNWs is still a big challenge. In this paper, we report the orientation-controlled growth of SiNW arrays on silicon (100), (111), and (110) substrates. The as-synthesized SiNWs are single-crystalline, with their axes lying along the [111] direction. Furthermore, almost every SiNW is naturally oriented perpendicular to one set of {111} planes of the substrate. As a result, the orientation of the SiNW array can be fully controlled by the crystal orientation of the substrate. These well-aligned SiNW arrays form regular networks on the substrate, and their orthographic projections on (100), (111), and (110) substrates form rectangular networks, triangular networks, and parallel straight lines, respectively. These regular nanowire networks are of great importance in constructing nanoscale electronic and photonic devices.

Forty years ago, Wagner showed that micrometer-sized silicon whiskers could be synthesized vertically on silicon substrates.[9,10] Recently, Yang and co-workers have also shown the vapor–liquid–solid (VLS) growth of well-aligned SiNW arrays.[11,12] They also mentioned the possibility of achieving precise orientational control of SiNW arrays by vapor–liquid–solid epitaxy (VLSE).[8] Here, we show that by carefully controlling the growth conditions, SiNWs can self-orient along the <111> directions of silicon substrates. As a result, the orientation of the SiNW arrays can be precisely controlled by the crystal orientation of the substrate. For our SiNW arrays synthesized on silicon (100) wafers, there are four fixed growth directions that make an angle of 35.3° with the substrate and correspond to the four equivalent <111> epitaxial directions of the substrate (Fig. 1). For (110) wafers, there are two equivalent growth directions that form an angle of 54.7° with the substrate (Fig. 2). Unlike the results of Wagner[9,10] and Yang,[11,12] whose whiskers or nanowires were all vertically aligned with the (111) substrate, our results show that SiNWs can grow along any one of the four <111> epitaxial directions of the (111) substrate (Fig. 3). At low supersaturation, SiNWs preferentially grow along the normal [111] direction, which is the same as Wagner and Yang's results. When the degree of supersaturation is large enough, SiNWs prefer the other three equivalent <111> directions that form an angle of 19.4° with the substrate. Four preferential growth directions appear simultaneously at intermediate supersaturation. These as-synthesized SiNW arrays can be directly employed for the construction of photonic devices, or be simply pressed onto the substrate to form regular nanoelectronic networks.

A conventional catalytic chemical vapor deposition process was employed to synthesize SiNWs. Thin gold films that were thermally evaporated onto silicon wafers served as the catalyst, while $SiCl_4$ vapor carried by hydrogen gas was the precursor. The growth of SiNWs followed a VLS mechanism.[11] A detailed description of this process can be found in the Experimental section.

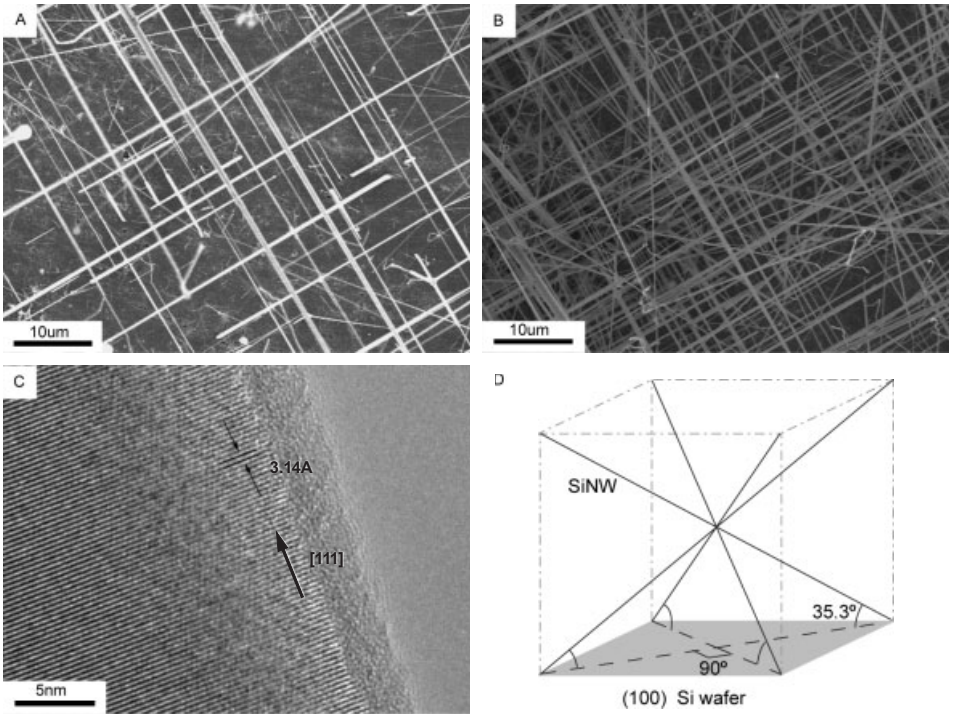

Figure 1. A,B) Scanning electron microscopy (SEM) images of the SiNW array grown on a Si (100) substrate. C) High-resolution transmission electron microscopy (HRTEM) image of an SiNW grown on the (100) substrate. The spacing of the lattice fringes is 3.14 Å. D) Schematic illustration of the four growth directions of the SiNWs on a Si (100) substrate. Solid lines represent the four growth directions of the SiNWs; they form an angle of about 35.3° with respect to the substrate. Dashed lines represent the projections of the SiNWs, which are perpendicular to each other.

ADVANCED MATERIALS

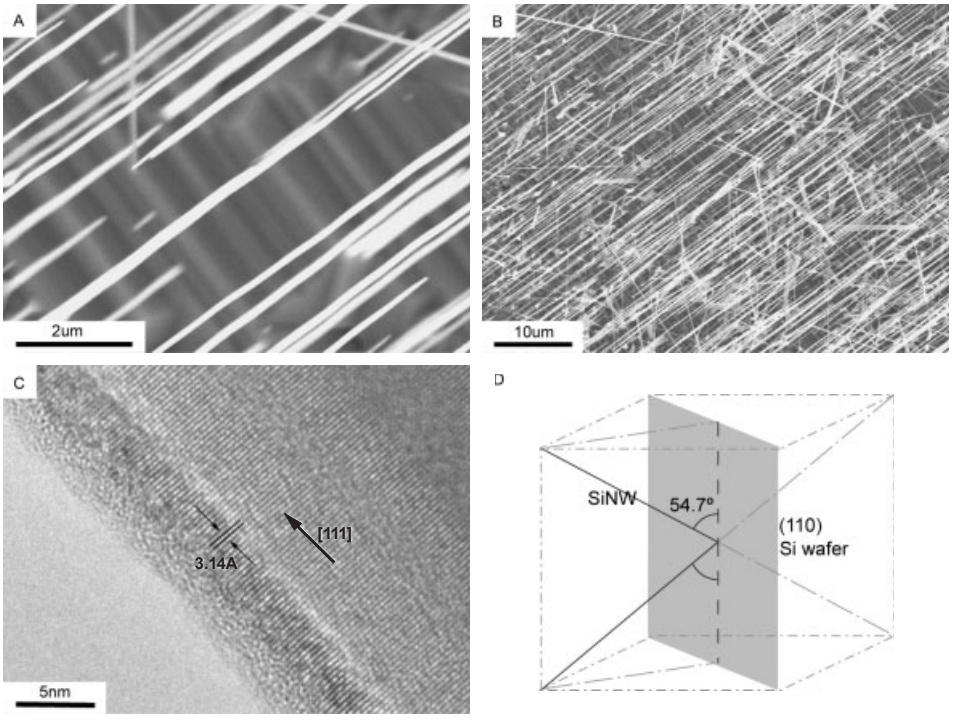

Figure 2. A,B) SEM images of the SiNW array grown on a Si (110) substrate. C) HRTEM image of an SiNW grown on the Si (110) substrate. The spacing of the lattice fringes is 3.14 Å. D) Schematic illustration of the two growth directions of SiNWs on a Si (110) substrate. Solid lines represent the two growth directions of SiNWs; they form an angle of about 54.7° with respect to the substrate. Dashed lines represent the projections of SiNWs on the substrate, which form parallel straight lines.

Rather unexpectedly, we found that even under the same experimental parameters, we obtained products with different morphologies in consecutive growth process. This phenomenon attracted our attention. One possible reason is that silicon deposition on the sidewall of the quartz tube is different in consecutive growth processes. We therefore conducted a further series of experiments to investigate this possibility. In these experiments, we kept all the experimental parameters fixed, including flow rates, furnace temperature, and growth time, as mentioned in the Experimental section. When we started a new series of experiments, we always cleaned the quartz tube to remove all the silicon deposits first, but didn't clean it again before the following growth runs. The order of growth runs appeared to be the key parameter for self-oriented growth of SiNWs. We denote each growth run by their order. For example, when we mention the "third growth", we mean that this growth run is the third one after the last cleaning of the tube. During the first growth, SiNWs vertically aligned on (111) substrates were synthesized (Fig. 3A), while no SiNWs were synthesized on the silicon (100) and (110) substrates. Self-oriented SiNW arrays (Figs. 1A,B, Figs. 2A,B, and Figs. 3B,C) were formed on (100), (110), and (111) substrates during the second and third growths. The fourth and later growths usually gave rise to large numbers of randomly oriented SiNWs (Fig. 3D). The self-oriented SiNWs are single crystalline, with their growth axes along the <111> direction (Figs. 1C,2C,3E); their diameters range from 50–250 nm (Figs. 1–3). All these results are repeatable for each series of growth runs.

Self-oriented SiNWs grown on a silicon (100) substrate are shown in Figure 1. Figures 1A,B show scanning electron microscopy (SEM) images taken from top views of the SiNW array on the (100) substrate. It is very clear that these SiNWs form rectangular networks. However, when the sample stage was tilted, we found that the SiNWs orient along four directions, forming an angle of about 35° with the substrates. Figure 1D illustrates the growth directions of the SiNWs grown on a silicon (100) substrate. These remind us that the silicon (100) substrate has four <111> directions at an angle of 35.3° to the surface of the substrate on which orthographic projections of these directions form rectangular networks. Hence, we deduced that the SiNWs grow along the <111> directions; this was subsequently confirmed by their high-resolution transmission electron microscopy (HRTEM) images (Fig. 1C).

Figure 2 shows self-oriented SiNWs grown on a silicon (110) substrate. Figures 2A,B are SEM images taken from top views of the SiNW array on the silicon (110) substrate. It appears that most of the SiNWs are parallel to each other. In fact, most of the SiNWs are oriented at an angle of about 55° to the substrates, and it is their orthographic projections on the substrate that are mutually parallel. Figure 2D illustrates the growth directions of the SiNWs, also corresponding to the <111> directions, which make an angle of 54.7° with the sili-

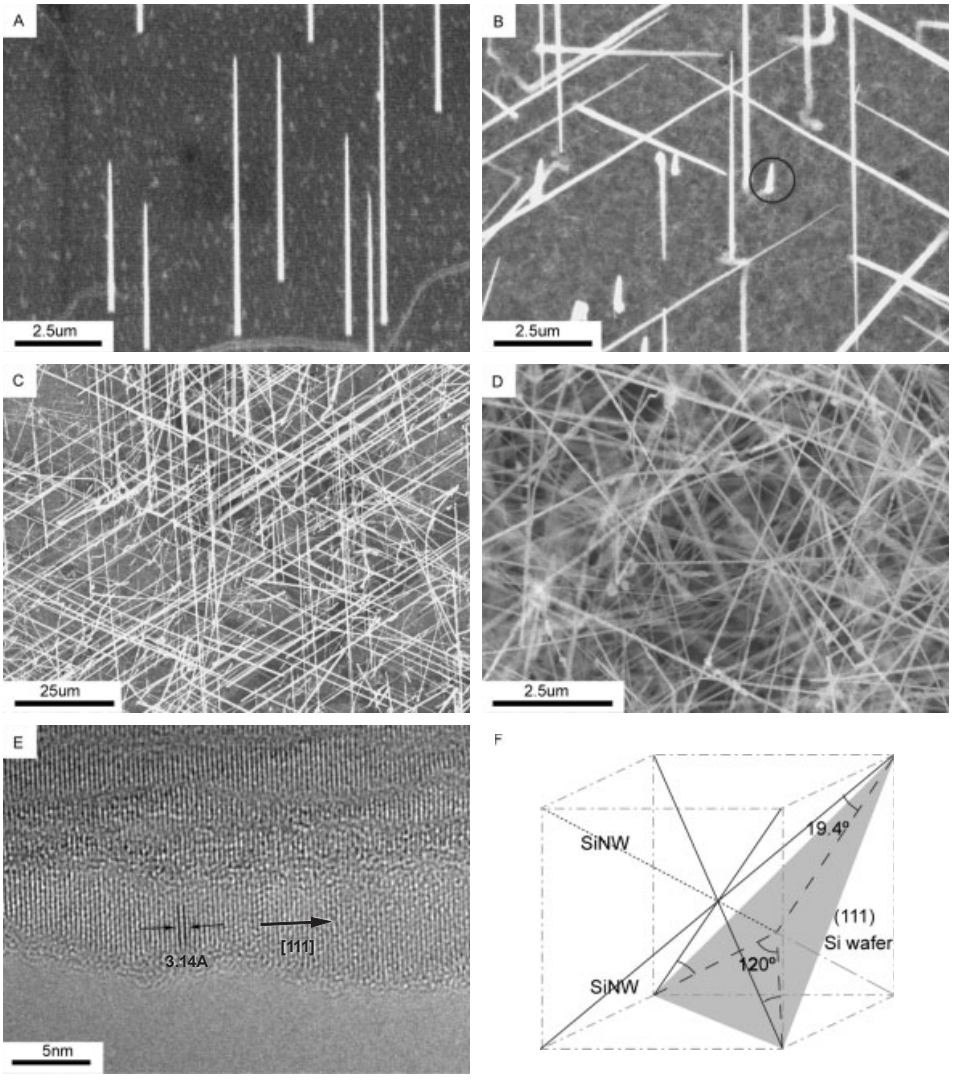

Figure 3. A) SEM image of the vertical SiNW array grown on a Si (111) substrate. B) SEM image of the SiNWs grown along four directions on a Si (111) substrate. The black circle indicates one of the vertical SiNWs. C) SEM image of the SiNWs grown along three directions forming an angle of 19.4° with respect to the Si (111) substrate. D) SEM image of the randomly oriented SiNWs. E) HRTEM image of a SiNW grown on the Si (111) substrate. The spacing of the lattice fringes is 3.14 Å. F) Schematic illustration of the four growth directions of SiNWs on a Si (111) substrate. The dotted line represents the direction perpendicular to the substrate, while the solid lines represent the three directions that form an angle of 19.4° with respect to the substrate, and the dashed lines represent projections of SiNWs on the substrate that form an angle of 120° with each other.

con (110) substrate. The HRTEM image (Fig. 2C) gives definite support for the [111] growth directions.

Figure 3 shows SiNWs grown on a silicon (111) substrate. Figure 3A is an SEM image (taken with the sample stage tilted by about 60°) of the SiNW array synthesized during the first growth. Nearly all the silicon nanowires are perpendicular to the substrate, as verified by the top-view image, in which the SiNWs are the light spots.

Figure 3B is an SEM image taken from nearly directly above the SiNW array synthesized during the second growth. Most of the SiNWs form triangular networks with some light spots (indicated by the black circle in the image) among them. Detailed observations indicate that most of the SiNWs are oriented along four directions, one of which is perpendicular to the substrate, with the other three at an angle of about 19° to the substrate. The light spots in the top-view image are the SiNWs perpendicular to the substrate.

Figure 3C is an SEM image showing the top view of the SiNW array synthesized during the third growth. Most of the SiNWs form triangular networks, and no light spots can be seen. In this case, the SiNWs are oriented mainly along three directions; SiNWs perpendicular to the substrate seem to be missing. Figure 3F illustrates the growth directions of the SiNWs: the dotted line represents the direction perpendicular to the substrate, and the solid lines represent the three directions that form an angle of 19.4° with the substrate. All four of these lines correspond to the <111> directions of the silicon (111) substrates. In summary, during the first growth only the

ADVANCED MATERIALS

growth direction indicated by the dotted line can be found, but during the second growth all four directions can be seen, and during the third growth only the three oblique directions indicated by the solid lines appear. All these growths appear to be epitaxial. The fourth and later growths give rise to randomly oriented SiNWs (Fig. 3D), and show no correlation with the crystal orientation of the substrate.

From the results listed above, it is evident that under some definite conditions, SiNWs predominately grow on silicon (100), (110), and (111) slices along the <111> directions of these substrates; this process is known as VLSE growth.[8] It is well-known that the growth of SiNWs promoted by metal impurities is based on a VLS mechanism.[11] In our experiments, each SiNW was capped with an Au catalyst, which implies an underlying VLS mechanism. For VLS growth of SiNWs, the nanowire diameter plays a crucial role in the growth direction.[13–15] For example, [111] is the preferential growth direction for large-diameter SiNWs[13,15] and whiskers.[10] The reason for this lies in the fact that a silicon atom precipitating upon the {111} surface during growth produces the largest decrease in Gibbs' free energy, because the {111} planes of silicon have the smallest separation and the largest density of surface atoms when acting as an interface.[16] When the diameter is very small, the free energy of the side faces must be taken into consideration.[15] As a result, [110] and [112] are the preferred growth directions for small-diameter SiNWs.[14,15] In our experiments, the diameters of the synthesized SiNWs are larger than 50 nm; therefore, most of them should grow along the <111> directions, as was verified by HRTEM.

Keeping in mind the fact that nearly all of our SiNWs grow along the <111> axes whether the growth is epitaxial or not, the question we must now consider is why under some conditions VLSE occurs, while other conditions give rise to randomly oriented SiNWs. Our results may give the answer. In our experiments, vertically aligned SiNWs grow during the first growth; oblique epitaxial growth takes place during the second and third growths; and the fourth and subsequent growths lead to randomly oriented SiNWs, which may be called non-epitaxial growth. What is the difference between these sequential growth runs? The answer may be the concentration of $SiCl_4$ in the growth zone. For the freshly cleaned quartz tube, most of the $SiCl_4$ has been deposited onto the sidewall of the quartz tube during the first growth, resulting in a decreased concentration in the growth zone. In the following growths, the deposition gradually decreases until equilibrium is reached. As a result, the actual concentration of $SiCl_4$ gradually increases to the preset value, which means the supersaturation in the successive growths is increasing.

It is well-known that crystal growth always begins with nucleation. According to the theory of crystallization,[17] nucleation induced by crystals is called "secondary" nucleation, whereas all nucleation in systems containing no crystalline matter is called "primary" nucleation. Primary nucleation that is induced by foreign particles is further classified as "heterogeneous" nucleation, while primary nucleation that occurs spontaneously is called "homogeneous" nucleation. Homogeneous nucleation usually needs the highest level of supersaturation. We believe it is the supersaturation level that determines whether the growth mode is epitaxial or non-epitaxial. According to the VLS mechanism,[10] the catalyst particle (Au in our case) and the silicon wafer underneath form a liquid-alloy droplet first. During this alloying process, the alloy droplet gradually dissolves the silicon atoms from the substrates until it reaches the equilibrium concentration of an Au–Si alloy at this temperature. The {111} planes dissolve more slowly for the same reason as for preferential growth in the <111> direction;[16] therefore, at the end of the alloying process, the droplet is supported by freshly formed {111} planes. These {111} planes can act as secondary nucleation sites at a low supersaturation level, which will result in epitaxial growth. When the supersaturation level is high enough, homogeneous nucleation can occur, which leads to the explosive growth of SiNWs.[10] This is the origin of non-epitaxial growth.

Compared with oblique epitaxial growth, vertical epitaxial growth of SiNWs on (111) substrates seems to be the most energetically favorable means of precipitating silicon atoms, hence it only requires the lowest supersaturation level. However, we still do not understand why this precipitation mode disappears during the third growth. More work is needed to clarify this point.

The ultimate goal of SiNW growth is to fabricate nanoscale photonic or electronic devices. Much effort has been devoted to assembling randomly oriented SiNWs onto substrates to make devices.[3,5] In the case of our VLSE-grown SiNW arrays, which have definite orientations, photonic devices can be directly fabricated by patterned growth of SiNWs without the need for further assembly procedures. Another attractive approach is to utilize the fact that the SiNW orthographic projections form rectangular networks on silicon (100) substrates, triangular networks on (111) substrates, and parallel straight lines on (110) substrates (Fig. 4). Direct pressing of the as-synthesized VLSE SiNW arrays produces planar rectangular networks, triangular networks, or parallel straight lines directly (Fig. 4), which can be further used in nanoelectronics.

In summary, the orientation-controlled growth of single-crystal SiNW arrays has been achieved by VLSE growth on silicon substrates. The orientation of the SiNW arrays can be

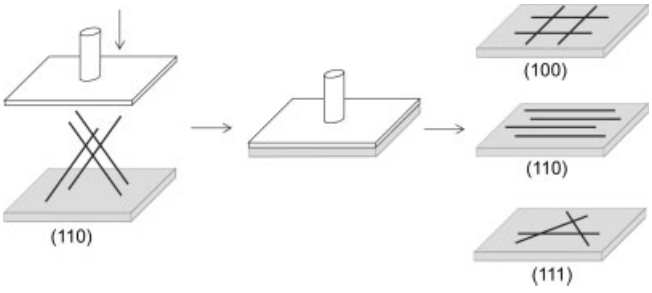

Figure 4. Schematic illustration of the formation of planar SiNW networks by pressing.

precisely controlled by the crystal orientation of the substrate. The nanowires are single-crystalline and grow in the <111> directions as determined by HRTEM. The SEM images show that almost every nanowire is aligned parallel to one of the <111> directions of the substrate. As a result, their orthographic projections form rectangular networks on silicon (100) substrates, triangular networks on silicon (111) substrates, and parallel straight lines on silicon (110) substrates. These self-oriented SiNW arrays could play a crucial role in fabricating nanoelectronic or nanophotonic devices, such as field emitters for flat-panel displays, nanoscale transistors, and photonic crystals.

Experimental

Au films (0.5–5 nm thick) were deposited on clean silicon (100), (110), and (111) wafers by thermal evaporation. These wafers were subsequently scribed into small pieces about 10 mm × 10 mm in size. In each experiment, one piece of (100), one piece of (110), and one piece of (111) were placed together into a ceramic boat, which was inserted into a long quartz-tube furnace at a fixed temperature of 900 °C (Fig. 5A). The quartz tube was then purged with 350 sccm of high-purity argon gas. After that, the quartz tube was gradually moved until the ceramic boat was in the center of the furnace

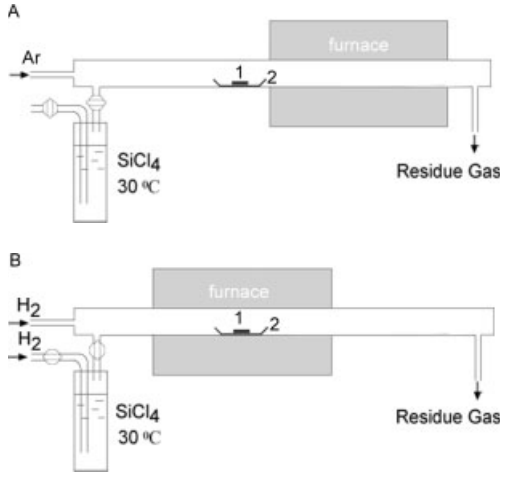

Figure 5. Schematic illustration of the experimental setup. A) Original position of Au-coated Si wafers (1) in ceramic boat (2). B) Position of boat during vapor-deposition process.

(Fig. 5B). When the temperature of the furnace reached 900 °C, the argon gas was substituted by 250 sccm of H_2, which served as the diluting gas. Then, another stream of hydrogen gas with a flow rate of 100 sccm was switched on as carrier gas. It was passed through a bubbler filled with liquid $SiCl_4$ (Alfa Aesar) held in an isothermal bath at 30 °C, thereby carrying saturated $SiCl_4$ vapor into the reaction zone. After 10 min reaction, the carrier gas and diluting gas were turned off, and the quartz tube was purged with 350 sccm Ar gas again. The quartz tube was then carefully moved back to its original position (Fig. 5A) so as to allow the ceramic boat to cool to room temperature.

The Si nanowire arrays were observed under a scanning electron microscope (SEM, JEOL JSM-6301F). An individual nanowire was viewed under a high-resolution transmission electron microscope (HRTEM, TECNAI F30) in order to characterize the crystal quality and growth direction.

Received: March 29, 2004
Final version: August 12, 2004

[1] G. Timp, R. E. Howard, P. M. Mankiewich, in *Nanotechnology* (Ed: G. Timp), Springer, New York **1999**, Ch. 2.
[2] Y. Xia, P. Yang, Y. Sun, Y. Wu, B. Mayers, B. Gates, Y. Yin, F. Kim, H. Yan, *Adv. Mater.* **2003**, *15*, 353.
[3] Y. Cui, C. M. Lieber, *Science* **2001**, *291*, 851.
[4] a) Y. Huang, X. Duan, Y. Cui, L. J. Lauhon, K. H. Kim, C. M. Lieber, *Science* **2001**, *294*, 1313. b) X. Duan, C. Niu, V. Sahi, J. Chen, J. W. Parce, S. Empedocles, J. L. Goklman, *Nature* **2003**, *425*, 274.
[5] X. Duan, Y. Huang, Y. Cui, J. Wang, C. M. Lieber, *Nature* **2001**, *409*, 66.
[6] a) M. H. Huang, S. Mao, H. Feick, H. Yan, Y. Wu, H. Kind, E. Weber, R. Russo, P. Yang, *Science* **2001**, *292*, 1897. b) J. C. Johnson, H. Yan, R. D. Schaller, L. H. Haber, R. J. Saykally, P. Yang, *J. Phys. Chem. B* **2001**, *105*, 11 387. c) X. Duan, Y. Huang, R. Agarwal, C. M. Lieber, *Nature* **2003**, *421*, 241.
[7] a) A. M. Morales, C. M. Lieber, *Science* **1998**, *279*, 208. b) D. P. Yu, Z. G. Bai, Y. Ding, Q. L. Hang, H. Z. Zhang, J. J. Wang, Y. H. Zou, W. Qian, G. C. Xiong, H. T. Zhou, S. Q. Feng, *Appl. Phys. Lett.* **1998**, *72*, 3458. c) Y. Yin, B. Gates, Y. Xia, *Adv. Mater.* **2000**, *12*, 1426. d) J. D. Holmes, K. P. Johnston, R. C. Doty, B. A. Korgel, *Science* **2000**, *287*, 1471. e) Q. Gu, H. Dang, J. Cao, J. Zhao, S. Fan, *Appl. Phys. Lett.* **2000**, *76*, 3020. f) T. Hanrath, B. A. Korgel, *Adv. Mater.* **2003**, *15*, 437. g) R. Q. Zhang, Y. Lifshitz, S. T. Lee, *Adv. Mater.* **2003**, *15*, 635. h) X. Zhang, L. Zhang, G. Meng, G. Li, N. Jin-Phillipp, F. Phillipp, *Adv. Mater.* **2001**, *13*, 1238. i) K. Peng, Y. Yan, S. Gao, J. Zhu, *Adv. Mater.* **2002**, *14*, 1164.
[8] Y. Wu, H. Yan, M. Huang, B. Messer, J. H. Song, P. Yang, *Chem. Eur. J.* **2002**, *8*, 1260.
[9] R. S. Wagner, W. C. Ellis, *Appl. Phys. Lett.* **1964**, *4*, 89.
[10] R. S. Wagner, in *Whisker Technology* (Ed: A. P. Levitt), Wiley, New York **1970**, Ch. 3.
[11] Y. Wu, R. Fan, P. Yang, *Nano Lett.* **2002**, *2*, 83.
[12] R. Fan, Y. Wu, D. Li, M. Yue, A. Majumdar, P. Yang, *J. Am. Chem. Soc.* **2003**, *125*, 5254.
[13] Y. Cui, L. J. Lauhon, M. S. Gudiksen, J. Wang, C. M. Lieber, *Appl. Phys. Lett.* **2001**, *78*, 2214.
[14] C. P. Li, C. S. Lee, X. L. Ma, N. Wang, R. Q. Zhang, S. T. Lee, *Adv. Mater.* **2003**, *15*, 607.
[15] Y. Wu, Y. Cui, L. Huynh, C. J. Barrelet, D. C. Bell, C. M. Lieber, *Nano Lett.* **2004**, *4*, 433.
[16] S. K. Ghandhi, *VLSI Fabrication Principles: Silicon and Gallium Arsenide*, 1st ed., Wiley, New York **1983**, Ch. 1.
[17] J. W. Mullin, *Crystallization*, 3rd ed., Butterworth-Heinemann, Oxford, UK **1997**, Ch. 5.

